

BUBBLES IN THE NORMAL AND STARBURST GALAXIES

S.A. Silich

Main Astronomical Observatory NAS of Ukraine,
03680, Kyiv-127, Golosiiv, Ukraine, *silich@mao.kiev.ua*

ABSTRACT. A kinetic feedback from massive stars on the interstellar medium (ISM) in normal and starburst (SB) galaxies is reviewed. Hot bubbles and expanding shells observational manifestations, and recent results from the numerical models are discussed. The possible reasons for hydrodynamic and X-ray discrepancies between the standard bubble model predictions and observations are analyzed.

Key words: Interstellar medium: Galaxies: Shock waves: Stellar winds: Supernova remnants.

1. Introduction

20 years have passed since the discovery by Heiles (1979) large empty cavities in the Milky Way neutral hydrogen distribution. Later on the study of interstellar bubbles has been extended to many nearby galaxies (see recent reviews by van der Hulst, 1996; Brinks & Walter 1998). The optical counterpart of these objects are the H_α ring-shaped nebulae (e.g. Meaburn 1980; Lozinskaya & Sitnik 1988). The similar structures have been also traced in the IR (Lozinskaya & Repin, 1990), and X-ray (Chu & Mac Low, 1990; Walter et al., 1998) emissions.

During the last two decades the major role of the radiative and kinetic feedback from massive stars on the distribution and physical conditions found in the ISM of the star forming galaxies has been well established. It is a general consensus (Tenorio-Tagle & Bodenheimer, 1988) that a majority of the observed structures originate from the combined action of stellar winds (SW) and supernova (SN) explosions in the massive star clusters (for the discussion of some potential problems see Gosachinskii, 1993; Rhode et al., 1999).

The observed shells can be tentatively classified into three distinct categories: small wind-blown or supernova produced bubbles around single individual stars (type S), moderate size bubbles, which result from the correlated action of a few to several hundreds of stars constituted a typical OB-association (type M), and huge superbubbles resulted from a violent, space correlated star forming activity in the SB galaxies (type H).

Table 1: Bubble classification.

Type	Progenitor	$\log(E/1 \text{ erg})$	Size (pc)
S	single star	51	~ 10
M	OB association	52-53	> 10
H	SB galaxy	≥ 54	≥ 1000

Our review will focus on the recent studies of the large-scale M and H type objects. A comprehensive discussions of the different aspects of the S bubble evolution one may found in the proceedings of the recent IAU Symposium N193 (e.g. Marston, 1999; Dopita et al. 1999).

A variety of different physical processes controls large bubbles evolution and observational manifestations: interstellar gas distribution, galaxy gravity and gaseous disc differential rotation, hot interior metal enrichment and cooling, hydrodynamical instabilities and effects of projection. Fast growth of our knowledge in this frontier field of the galaxy astrophysics was inconceivable without development of the suitable 2D and 3D numerical methods that are easy to work with, fast, and could give reasonable accuracy. Therefore I first briefly discuss one of the method based on the thin layer approximation we have developed during the last decade. Then I discuss the effects of projection, Large Magellanic Cloud (LMC) M-bubbles growth rate discrepancy, the origin of the $Ly\alpha$ profiles in the starburst galaxies. At the end of the presentation I turn to the bubble X-ray emission, a particularly exiting topic in view of the new AXAF and XMM missions.

2. Thin layer approximation

An impressive progress in our knowledge of the energetic processes that make up ISM, has been made with the development of the multidimensional hydrodynamical methods. First analytic approximation for a two-dimensional adiabatic shock wave propagation within an exponential, plane-stratified gas density distribution, has been proposed by Kompaneets (1960). Later on Kompaneets approach has been improved to take

into account the inertia of the post-shock expanding shell (Andriankin et al., 1962). This version of the Kompaneets method is known as a thin layer approximation, and is widely used in a number of astrophysical applications (see for review Bisnovatyi-Kogan & Silich, 1995).

First 2D numerical scheme based on the thin layer approximation has been developed by Bisnovatyi-Kogan & Blinnikov (1982), who has applied this method for SNRs resulting from asymmetric, plane concentrated supernovae ejecta. Later on Tenorio-Tagle & Palouš (1987), Mac Low & McCray (1988) have used a similar approach to discuss M-type bubble evolution in a plane-stratified, differentially rotating galaxy disk. Mac Low et al. (1989), Bisnovatyi-Kogan et al. (1989) have compared the thin layer approximation results with the analytic and full numerical calculations and did confirm their good accuracy.

3D numerical schemes based on the thin layer approach have been developed independently by Bisnovatyi-Kogan & Silich (1991), Silich (1992) and Palouš (1992) (see for review Bisnovatyi-Kogan & Silich, 1995). In this approach shock is approximated with a number of Lagrangian elements. If m is the mass, \mathbf{r} is the radius-vector, \mathbf{u} is the velocity of the particular Lagrangian element, and $\rho(x, y, z) = \rho_0 f(x, y, z)$ is the ambient gas density, then equations of the mass and momentum conservation may be written as follows:

$$\frac{dm}{dt} = \rho(x, y, z)(\mathbf{u} - \mathbf{V})\mathbf{n}\Sigma, \quad (1)$$

$$\frac{d}{dt}(m\mathbf{u}) = \Delta P\mathbf{n}\Sigma + \mathbf{V}\frac{dm}{dt} + m\mathbf{g}, \quad (2)$$

$$\frac{d\mathbf{r}}{dt} = \mathbf{u}, \quad (3)$$

where \mathbf{n} is the normal to the shock front unit vector, \mathbf{g} is the acceleration of the external gravitational field, \mathbf{V} is the velocity field of the external gas flow, Σ is the surface area of the Lagrangian element, $m = \sigma\Sigma$, σ is the surface density, and $\Delta P = P_{in} - P_{ext}$ is the pressure difference between the hot interior and rather cold external gas. The pressure P_{in} is a function of the bubble thermal energy E_{th} and remnant volume Ω :

$$P_{in} = (\gamma - 1)E_{th}/\Omega. \quad (4)$$

The motion of any Lagrangian element is then described by seven ordinary differential equations. For N Lagrangian elements one gets a system of $7N$ differential equations of the mass and momentum conservation. This set of equations is coupled by the equation (4) for the gas pressure within a cavity, and the energy conservation equation. Numerical integration of these equations gives time evolution of a shell shape, expansion velocity, and surface density distribution. The results of the calculations for the superbubble evolution

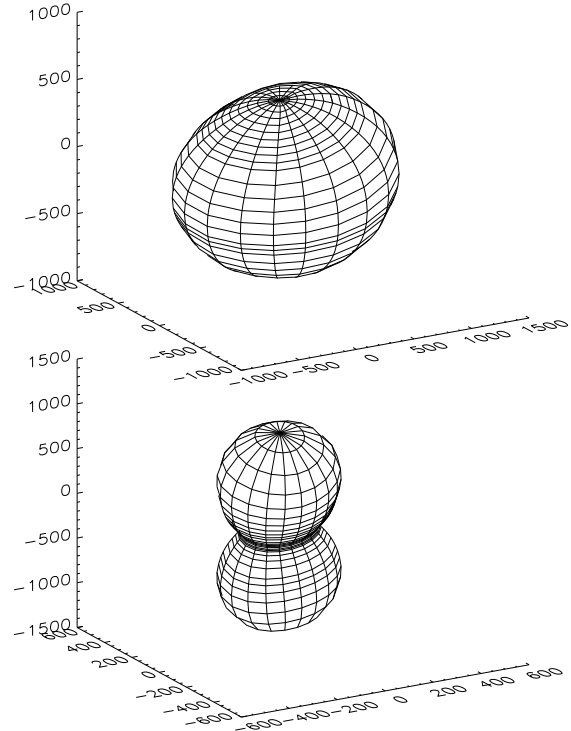


Figure 1: Bubble morphology for HoII (top), and M31 (bottom) galaxies.

in the M31 and HoII galaxies are shown in figure 1 (Silich et al., 1996).

2. The projection effects

The growing bulk of observational data and fast progress in numerical methods led to a new understanding of the ISM as a dynamic system regulated by a number of local energy sources. However, the development of the *quantitative* theory has required to provide numerous calculations and compare their results with observational data.

As soon as most of the objects were found in the external galaxies, a principal problem arisen: how to distinguish between the distortion effects of projection and bubble real 3D morphology? Silich et al. (1996), Mashchenko & Silich (1997) incorporated effects of projection into their 3D numerical scheme, and provided a careful analysis of the problem for neutral hydrogen shells. From the observational point this problem was analysed by Thilker et al. (1998). Later on Mashchenko et al. (1999) have incorporated the thin layer numerical model into Thilker et al. (1998) method for automated identification and classification of supershells in the spiral galaxies.

Search for the neutral hydrogen shells in the external spiral and irregular galaxies includes analysis both of integrated, and single velocity neutral hydrogen maps. For example, it was found that in IC 2574 neutral

hydrogen holes are more prominent in the single velocity channels, whereas in the HoII it is easier to identify the same objects in the integrated column density map (Brinks & Walter, 1998).

Let us define the galaxy reference system (x, y, z) , and the coordinate system (x', y', z') in the plane of view. The HI column density along any line of sight follows from the equation:

$$N(x', y') = \sum_l N_l + \int n(x', y', z') dz', \quad (5)$$

where index l denotes different Lagrangian elements along line of sight, and N_l is the contribution of each Lagrangian element to the total column density. The last term represents the galactic cold ISM contribution. The value of shell contribution, N_l , depends on the shell column density, N_{sl} , shell thickness, d , and angle, α , between the line of sight and the normal to the shell surface (Silich et al., 1996):

$$N_l = \frac{N_{s,l}}{\delta} \times \begin{cases} F_1(\alpha, \beta) - F_2(\alpha, \beta), & \alpha < \alpha_{cr}, \\ 2 F_1(\alpha, \beta), & \alpha \geq \alpha_{cr}, \end{cases} \quad (6)$$

where $\delta = d/R_s$ was assumed to be constant, d and R_s are the shell thickness and radius.

$$F_1(\alpha, \beta) = \sqrt{\cos^2 \alpha + \delta + \frac{\delta^2}{4}}, \quad (7)$$

$$F_2(\alpha, \beta) = \sqrt{\cos^2 \alpha - \delta + \frac{\delta^2}{4}}, \quad (8)$$

A careful analysis of more than 10000 models reveals that projection effects are highly dependant not only on the inclination angle i , but also on the bubble position in the plane of a galaxy. A projection distortion is negligible nearby galaxy major and minor axes, but dominates hole orientations in the intermediate sectors. These results made it possible to propose a new method which can distinguish between the two possible directions (towards and outwards of observer) of the galactic angular momentum vector, the problem which is close related with the physical conditions at the epoch of galactic formation.

Mashchenko & Silich (1997) extended this study on the different velocity channels. They introduced Gaussian sensitivity curves for spectral filters:

$$W(U, \sigma_f) = \frac{1}{\sigma_f \sqrt{2\pi}} \exp \left\{ -\frac{1}{2} \left[\frac{U - V}{\sigma_f} \right]^2 \right\}. \quad (9)$$

where V is the central velocity, and σ_f is dispersion of a particular filter. Then number of neutral hydrogen atoms on the line of sight reads as:

$$N_j = \frac{1}{\sigma_* \sqrt{2\pi}} \int_{-\infty}^{\infty} n(z') \exp \left\{ -\frac{1}{2} \left[\frac{V(z') - V_j}{\sigma_*} \right]^2 \right\} dz', \quad (10)$$

Where $\sigma_* = \sqrt{\sigma_f^2 + \sigma_g^2}$, σ_g^2 is the ISM gas random motion one-dimensional velocity dispersion. Finally, to imitate radiotelescope spatial resolution, this value was smoothed with a two-dimensional Gaussian function. New algorithm was applied for several supershells in the M31 and HoII galaxies. The calculations revealed a principal role of the ISM gas random motion, and an interesting effect of the hole center displacement at the different velocity channels. These results have to be taken into account at any analysis of observational data to avoid misinterpretation of the same object as several intersecting or overlapping shells.

4. Bubble dynamic discrepancy

Due to it's proximity and almost face-on position the Large Magellanic Cloud (LMC) provides an excellent possibility to study a multi-shell structure of the ISM, and interstellar hydrodynamic state around individual OB-associations. It is important to note, that the LMC internal and foreground extinction is so small, that detailed studies of the LMC OB-associations stellar contents are now easy possible (Saken et al., 1992; Oey 1996a). These photometric and spectral observations in combination with the stellar evolution models constrain all input model parameters one needs to compare the observed objects with the bubble model predictions: bubble sizes, expansion velocities, and mechanical energy input rate.

This comparison (Oey, 1996b) indicates, that the standard spherical model cannot reproduce the observed properties of a number of shells. In particular, the collection of bubbles observed in the LMC exhibit two different sets of objects with expansion velocities that are either too high or too low to be explained by the standard model. For the low velocity objects, the discrepancy could probably be explained by errors in the estimation of the input wind power or ambient gas density (Oey 1996b). For the high velocity shells, however, the observed expansion velocities ($V_{exp} \geq 25$ km s⁻¹) are at least a factor of two larger than the expected values (Oey 1996b). These objects are rather young. Their radii fall in the range 25 - 50 pc, and lifetimes are several Myrs. Neither the density gradient in the disk of the LMC nor possible variations of the initial stellar population can resolve this discrepancy (Oey 1996b).

A possible solution to this problem has been suggested by Silich & Franco (1999). It is based on the fact that the LMC has a moderate inclination angle, and therefore LMC shells are viewed with a nearly face-on orientation. It is well-known, that in the plane-stratified gas density distribution shock wave exhibits at first a continuous deceleration, and only when top radius exceeds several characteristic scales of gaseous

disc thickness, top expansion changes towards the increasing speed. It is clear that LMC bubble large expansion velocities cannot be related to a large-scale density gradient. The observed shells are too small to blowout of the LMC gaseous layer. Shell acceleration could be pronounced only if one takes into account the presence of a giant molecular cloud (GMC) which gives birth to the parental stellar cluster and controls the initial bubble expansion. The high initial mass concentration induces strong changes in the young bubble dynamics. There is a bulk of the observational evidences which indicate that GMCs are rather flat than spherically symmetric objects (e.g. Gosachinskii, this volume). Therefore a simple two-dimensional model for a GMC surrounded by a homogeneous ISM was considered:

$$\rho = \begin{cases} \rho_c, & F(r, z) \leq 1, \\ F(r, z)^{-w/2}, & F(r, z) \leq \xi^{2/w}, \\ \rho_{ISM}, & F(r, z) > \xi^{2/w}, \end{cases} \quad (11)$$

where $F(x, z) = \left(\frac{r}{R_c}\right)^2 + \left(\frac{z}{Z_c}\right)^2$, $\xi = \rho_c/\rho_{ISM}$ is the ratio of the cloud core density to the ISM gas density, w is the power-law index, and R_c and Z_c are the characteristic scale heights for the cloud density distribution in the r and z -directions, respectively. The appropriate range of values for the cloud parameters was derived from observational data, and cloud flatness $Z_c = R_c/2$ was assumed.

Figure 2 presents the results of the calculations for $2 \times 10^4 M_\odot$ cloud with different mass concentrations at the cloud center (a low-density cloud with $n_c = 10 \text{ cm}^{-3}$, and high density cloud with $n_c = 10^2 \text{ cm}^{-3}$).

These results indicate that bubbles blowing out of the flattened clouds can reach a high degree of asymmetry on a short time scale (during the first million years of expansion), with z -velocities in the range of the observed high-velocity cases. The model considered predicts a remarkable difference in the bubble kinematics for a face-on and edge-on galaxies, and is in line with the semi-analytical results for a sharp density contrast discussed by Oey & Smedley (1998).

5. Ly α profiles in the SB galaxies

It has been long proposed that primordial galaxies have to be easy detected from their Ly α emission. However ultraviolet (UV) observations of high redshifted galaxies show that many of them present weak, or sometimes none Ly α emission at all (Lowenthal et al., 1997). This problem puzzled the astronomical community for more than a decade, and stimulated many discussions and new observational programs. Recent HST data on star-forming galaxies (see e.g. Kunth et al., 1998) revealed three typical Ly α profiles: broad damped absorption, pure emission, and emission with

P Cygni type blueshifted absorption. Sometimes the additional details like emission within a damped absorption, or redshifted emission are also observed. P Cygni absorptions have rather large (several hundred km s^{-1}) offset with respect to the parent galaxy. These observations lead to suggestion, that the velocity field and ISM density distribution along line of sight, rather than dust absorption alone, are the dominant factor for the escape of the Ly α photons from these galaxies.

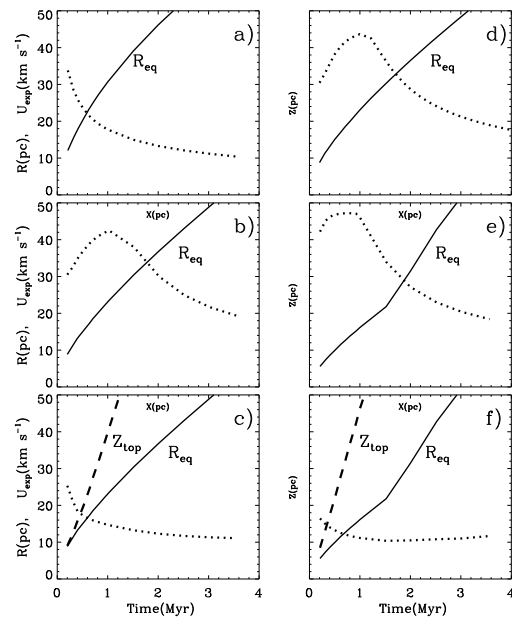


Figure 2: Bubble expansion from a GMC. a) Spherical cloud. b) Low density cloud as seen in a face-on galaxy. c) Low density cloud as seen in an edge-on galaxy. d) Low density cloud with shell fragmentation due to R-T instability. e) High density cloud for a face-on galaxy. f) High density cloud for an edge-on galaxy. The solid lines are the shell radii along the plane of the galaxy, and the dashed lines are the top z -extensions. Dotted lines for panels a, b, d and e are the top expansion velocities along the z -axis. Dotted lines for panels c and f are the expansion velocities at the bubble equator.

A qualitative scenario for different Ly α profile origin was proposed by Tenorio-Tagle et al. (1999). The model is based on the synthetic properties of starbursts, as derived by Leitherer & Heckman (1995), and considers the galaxy ISM hydrodynamic response on the SB mechanical energy deposition $L_{SB} = 10^{38} - 10^{42} \text{ erg s}^{-1}$. The ISM gas distribution was approximated with the two isothermal components related to the central dense molecular core, and low density extended gaseous halo

$$\rho_g = \rho_{core} + \langle \rho_{halo} \rangle \quad (12)$$

retained in an equilibrium state by rotation, random gas motion, and gravity from the stellar and dark mat-

ter components. It was assumed, that ISM constitutes 10% of the total mass of the galaxy, and ranges from $5 \times 10^7 M_\odot$ for smallest dwarf galaxies to the $10^{10} M_\odot$ for the massive spiral ones.

The numerical code described in the section 2, was completed with the algorithms which define a shell thickness, and Stromgren zone extension. The Stromgren zone radii were calculated in the equilibrium on-the-spot, radial approximation with account for gas concentration within a high density shell:

$$\Delta(R) = N_{UV} - 4\pi \left(\int_{R_1}^{R_2} n^2(r) \alpha_B r^2 dr - \int_{R_2}^R n^2(r) \alpha_B r^2 dr \right), \quad (13)$$

where R_1 and R_2 are the inner and outer shell cross points along line of sight, $\alpha_B = 2.59 \times 10^{-13} \text{ cm}^3 \text{ s}^{-1}$ is the recombination coefficient of the hydrogen atoms to all levels but the ground state. If value of Δ is positive

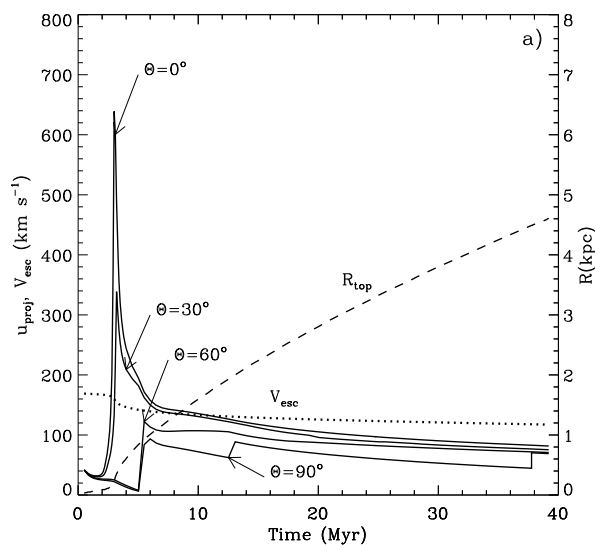


Figure 3: Bubble time evolution. Solid lines represent the expansion velocities along different line of sights. Dotted line indicates the local escape velocity. Bubble pole position is indicated by the dashed line.

at the galaxy boundary R_G , there are enough UV photons to ionize neutral hydrogen shell, all interstellar gas along line of sight, and escape of the galaxy. If value of $\Delta(R_G)$ is negative, the number of UV photons is not sufficient to ionize all the halo. The radius of the HII region follows from the condition $\Delta(R) = 0$, and lies between the shock front and the galaxy outer boundary R_G . Note, that the characteristic recombination time $\tau_{rec} = 1/n_e \alpha_A \approx 10^5/n_{halo}$ yr of the low density halo may exceed bubble expansion time t . This causes the ionized halo to become temporarily transparent to the

$\text{Ly}\alpha$ photons, even upon dramatic drop of the central UV flux, which is expected after 4 - 5 Myr in the instantaneous SB model. The hydrodynamical evolution of the typical model is shown in the figure 3.

The shell expansion shows at first continuous deceleration, followed after 1 - 2 Myrs by a sudden blowout with rapid acceleration and Rayleigh-Taylor disruption of the pole sections. Later on the shock builds a new shell of swept-up halo matter. The remnant speed begins to decline, and ends up well below the galaxy escape velocity. Nevertheless, after 20 - 40 Myr a SB forms a huge, several kiloparsec size remnant filled with a low density ($10^{-3} - 10^{-4} \text{ cm}^{-3}$) hot gas, which is surrounded by a massive, rather cold shell.

Before the blowout the dense, slowly expanding shell preserves interstellar gas of the powerful ionizing radiation, which escape of the central star forming region. However, after blowout UV photons escape of the disrupted pole segments, and produce a cone of ionized interstellar gas around the symmetry axis Z. This cone becomes rapidly broader, and reaches its maximum opening angle after 2.5 - 3 Myr (figure 4).

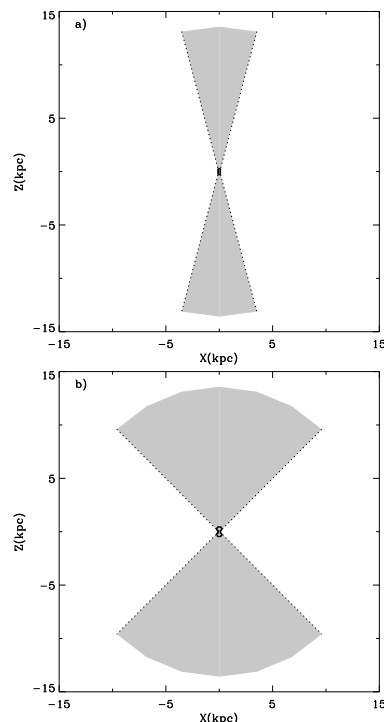


Figure 4: The development of the conical HII region in the low density galaxy halo.

The rapid changes in the ionization state of the galaxy ISM have a profound impact on the transport of the $\text{Ly}\alpha$ emission, and lead to a sequence of the $\text{Ly}\alpha$ profiles. This sequence starts with a broad damped absorption, which followed after blowout by a pure emission. Recombinations in a totally ionized new-formed shell produce a secondary blue-shifted emission. However, if the shell column density grows to $\sim 10^{19} \text{ cm}^{-2}$, it

traps the ionization front, and forms a multiple structure with a photoionized inner edge, a central neutral zone, and outer collisionally ionized layer. This is promoted also by the rapid decrease in the UV production rate after 3 - 4 Myrs, and UV flux geometrical dilution. Once the neutral hydrogen zone is formed, the recombinations within a shell become increasingly more important, leading to a P Cygni Ly α profile and eventually again to a full saturated absorption.

5. Hot gas and X-ray emission

Search for hot gas within the neutral hydrogen shells is an important test of the standard (space correlated supernova explosions within a young stellar cluster) model. LMC provided an excellent laboratory for this purpose during Einstein and ROSAT observatories epoch. With the AXAF and XMM launch this research will be extended on a number of the nearby galaxies, and new exiting results are expected in the forthcoming few years.

Interstellar bubbles with cold radiative shells and adiabatic interiors have four zone structure (Weaver et al., 1977). A central zone containing a freely expanding wind matter. Hot interior zone which is filled with a gas heated at the inner reverse shock. This zone is bounded with a cold shell, which is separated by a contact discontinuity and accumulates swept-up interstellar gas. This zone is bounded with a leading shock front, which separates a bubble shell of the external ISM. Second zone covers most of the bubble volume. It contains mixture of the heated at the reverse shock ejecta and evaporated from a cold shell interstellar gas. This mixture has temperatures of $10^6 - 10^7$ K, and produce bulk of the X-ray emission. Note, that in the low density environment (or at a very high energy input rate) bubble shell remains adiabatic for a long time, and also contributes to a bubble total X-ray luminosity.

A simple analytic model for X-ray luminosity L_x from a spherically symmetric, energy dominated bubble with a cold radiative shell, has been developed by Chu & Mac Low (1990) for a constant energy input rate, and Silich (1995) for a power law energy deposition. This model is based on the self-similar hot inner gas temperature and density distributions (Weaver et al., 1977), accounts for a X-ray emission cut-off temperature $T_{cut} \sim 5 \times 10^5$ K, and approximates X-ray emissivity within the 0.1 - 2.4 keV energy band by a constant value $\Lambda_x = 3\xi \times 10^{-23}$ erg cm 3 s $^{-1}$, where ξ is the hot gas metallicity in the solar units. A simple analytic expression may be derived for a constant ambient gas density n_0 , and constant mechanical energy input rate L_w :

$$L_x = 10^{36} \xi I(\tau) L_{38}^{33/35} n_0^{17/35} t_7^{19/35} \text{ erg s}^{-1} \quad (14)$$

where L_{38} is wind mechanical luminosity in the 10^{38} erg s $^{-1}$ units, and t_7 is the elapsed time in the 10^7 yr unites. $I(\tau)$ is a dimensionless integral:

$$I(\tau) = \frac{125}{33} - 5\tau^{1/2} + \frac{5}{3}\tau^3 - \frac{5}{11}\tau^{11/2}, \quad (15)$$

and τ is the ratio of the X-ray cutoff temperature to the bubble central one. More comprehensive numerical models, which account for bubble deviation of the spherical symmetry, and use equilibrium Raymond & Smith (1977) model for the X-ray emissivity, have been developed for Milky Way bubbles by Silich et al. (1996), and SB bubbles by Suchkov et al. (1994), Silich & Tenorio-Tagle (1998), Strickland & Stevens (1999).

To date X-ray emitting, shocked stellar wind bubble from a single star has been unambiguously detected in the only one object NGC 6888 (Bochkarev, 1988, Wrigge et al., 1994) while a number of the X-ray emitting M and H-type objects grows continuously.

Chu & Mac Low (1990) have examined Einstein Observatory archives, and revealed diffuse X-ray emission around 15 LMC OB-associations. The regions with X-ray excess correlate with the H α emission, and best can be associated with the hot M-type bubbles. Bubble X-ray luminosities range from 7×10^{34} to 7×10^{36} erg s $^{-1}$. The comparison of the observed values with the model predicted ones revealed an intrigue result: X-ray bright bubbles have X-ray luminosities more than an order of magnitude higher than model predicted ones. Later on this result has been confirmed with the ROSAT data (Chu et al., 1993). Several X-ray dim M-bubbles were also found (DEM 31, DEM 105, DEM 106, and DEM 137) in the LMC survey (Chu et al., 1995). In these cases 3σ upper limits are comparable with the model predicted ones, but deeper exposure, or more sensitive observations are needed to determine their real X-ray luminosities.

30 Dor, the most spectacular HII nebula in the Local Group of galaxies, provides an excellent possibility for understanding massive star origin and its interaction with the ISM. The central OB-association, NGC 2070, was formed 1 - 2 Myr ago, and emits $\sim 10^{52}$ UV photons every second. HII filaments extend more than 100 pc away of the cluster, and coincide with the regions of the diffuse X-ray emission. Two high mass binaries and supernova remnant N157B have been revealed in the 30 Dor core region (Wang, 1999). However, X-ray emission is predominantly diffuse, and ASCA data confirm its thermal origin. The best estimation of the emitting gas temperature in the two-component model gives value in the $2 - 9 \times 10^6$ K range, and intrinsic X-ray luminosity in the 0.5 - 2 keV energy band of $L_x \approx 9 \times 10^{37}$ erg s $^{-1}$ (Wang, 1999). This low temperature indicates on the additional mass ejection into a cavity, which is likely to be an effective erosion of the parent molecular cloud via photoevaporation from the central compact star cluster.

Several huge (kiloparsec scale) regions of the diffuse X-ray emission in the LMC coincide with the well known HII giant shells LMC-4 and LMC-2 (Bomans et al., 1996, Caulet & Newell, 1996). Walter et al. (1998) have revealed a similar (1000×500 pc) in size object in the nearby dwarf galaxy IC 2574. An X-ray excess coincides with the HI shell in the northeast part of this galaxy, and the region of the star-forming activity as traced by the H α emission. The observed X-ray luminosity in the 0.1 - 2.4 keV energy band is $L_x \approx 1.6 \times 10^{38}$ erg s $^{-1}$. It is suggested that main contribution comes from the hot gas embedded within a shell, although contamination from the X-ray binaries cannot be ruled out. Simple estimations show that this luminosity is about an order of magnitude higher than those, which predicted by the theoretical model (14). The same problem, as has been discussed above for the most X-ray emitting bubbles in the LMC.

ROSAT observations one of the most X-ray luminous ($L_x \sim 10^{40}$ erg s $^{-1}$) dwarf galaxy HoII present opposite problem. Despite of violent ISM structure with a number of neutral hydrogen holes and expanding shells (Puche et al., 1992), main X-ray emission comes from a single unresolved region, which coincides with a large HII region. A high X-ray variability supports accretion into a compact object rather than extended bubble model (Zezas, 1999).

Star formation activity gets its extreme value in the starburst galaxies. These systems are between the brightest sources of the IR emission, present obvious evidences for the powerful gas outflow in the visible wave length band, and also often present the extended (tens of kiloparsecs) diffuse X-ray emission. To date only several dwarf and peculiar galaxies have definite detection of extended, thermal X-ray emission (Martin, 1999). There are NGC 1569 NGC 4449, M82. Several others, NGC 5253, NGC 4214, NGC 1705, I Zw18, have been also detected in the X-ray band, but interpretation of the existing data is controversial (for a comprehensive analysis see Strickland & Stevens, 1998). For a example, Martin & Kennicutt (1995) found, that the observed X-ray luminosity of NGC 5253 ($L_x \sim 6.5 \times 10^{38}$ erg s $^{-1}$) exceeds standard bubble model predictions more than an order of magnitude.

6. Conclusions

Interstellar bubbles present direct manifestation of massive star cluster feedback on the galaxy ISM, and have profound importance to the global galaxy structure, star formation history, chemical evolution, energy balance, and relationship between different gaseous phases.

Several potential problems with this hypothesis, however, are waiting for their intensive discussion. The basic ones may be formulated as follows:

- A comprehensive study of the stellar population within the large (M and H-types) bubble regions. Search for the excess of the late (A, F) type stars, the debris of the initial massive star clusters.
- Extension of the LMC analysis of the bubble kinematics on the another nearby face-on and edge-on galaxies. The comparison of the coherent SNe model predictions with a variety of observational data.
- A detailed analysis of the different mechanism which may be responsible for superbubbles X-ray emission: off-center SN explosions, mass-loading flows, hot gas metal enrichment, etc. New series of the X-ray observations of the nearby normal and SB galaxies with better sensitivity and space resolution.

Acknowledgements. It is my please to acknowledge support from a Royal Society grant for joint projects with the former Soviet Union states. I am also greatly appreciate many useful discussions of the reviewed problems with my colleagues and friends: G. Bisnovatyi-Kogan, J. Franco, T. Lozinskaya, R. Terlevich and E. Terlevich, G. Tenorio-Tagle.

References

- Andriankin, E.I., Kogan, A.M., Kompaneets, A.S. and Krainov V.P.: 1962, *Zh. Prikl. Mekh. Tekh. Fis.*, **6**, 3.
- Bisnovatyi-Kogan G.S., Blinnikov S.I.: 1982, *Astron. Zh.*, **59**, 876.
- Bisnovatyi-Kogan G.S., Blinnikov S.I., Silich S.A., 1989, *Ap&SS*, **154**, 229.
- Bisnovatyi-Kogan G.S., Silich S.A.: 1991, *Astron. Zh.*, **68**, 749.
- Bisnovatyi-Kogan G.S., Silich S.A.: 1995, *Rev. Mod. Phys.*, **67**, 661.
- Bochkarev N.G. 1988, *Nature*, **332**, 518.
- Bomans D.J., De Boer K.S., Koornneef J., Grebel E.K.: 1996, *Astron. Astrophys.*, **313**, 101.
- Brinks, E., Walter, F.: 1998, in *The Magellanic Clouds and Other Dwarf Galaxies*, ed. T. Richtler & J. Braun (Aachen: Shaken Verlag), p.1.
- Caulet A., Newell R.: 1996, *Astrophys. J.*, **465**, 205.
- Chu Y.-H., Mac Low M.-M.: 1990, *Astrophys. J.*, **365**, 510.
- Chu Y.-H., Mac Low, M.-M., Garsia-Segura G., Wakker B., Kennicutt R.C.: 1993, *Astrophys. J.*, **414**, 213.
- Chu Y.-H., Chang H.-W., Su Y.-L., Mac Low M.-M. 1995, *Astrophys. J.*, **450**, 157.
- Dopita M.A., Kim M.S., Oey M.S., Lozinskaya T.A. 1999, in IAU Symposium N193 *Wolf-Rayet phenomena in massive stars and starburst galaxies*, eds. K.A. van der Hucht, G. Koenigsberger & P.R.J. Ee- nens, p.441.

- Gosachinskij I.V.: 1993, in ASP, **66**, *Physics of the gaseous and stellar disks of the Galaxy*, ed. I.R. King, 257.
- Heiles C.: 1982, *Astrophys. J.*, **262**, 135.
- Kompaneets A.S.: 1960, *Doklady Akad. Nauk SSSR*, **130**, 1001.
- Leitherer C., Heckman T.M.: 1995, *Astrophys. J. S.*, **96**, 9.
- Kunth D., Mas-Hesse J.M., Terlevich E., Terlevich R., Lequeux J., Fall M.: 1998, *Astron. Astrophys.*, **334**, 11.
- Lozinskaya T.A., Sitnik, T.G.: 1988, *Astron. Zh. Letters*, **14**, 240
- Lozinskaya T.A., Repin S.V.: 1990, *Astron. Zh.*, **67**, 1152
- Mashchenko S.Ya., Silich S.A., 1997, *Astron. Zh.*, **74**, 25.
- Mashchenko S., Thilker D., Braun, R.: 1999, *Astron. Astrophys.*, **343**, 352.
- Mac Low M.-M., McCray R.: 1988, *Astrophys. J.*, **324**, 776.
- Mac Low M.-M., McCray R., Norman N.L.: 1989, *Astrophys. J.*, **337**, 141.
- Marston A.P.: 1999, in IAU Symposium N193 *Wolf-Rayet phenomena in massive stars and starburst galaxies*, eds. K.A. van der Hucht, G. Koenigsberger & P.R.J. Eenens, p.306.
- Martin C.L., Kennicutt R.C.: 1995, *Astrophys. J.*, **447**, 171.
- Martin C.L.: 1999, *Astrophys. J.*, **513**, 156.
- Meaburn, J. 1980, *Mon. Not. R. Astron. Soc.*, **192**, 365.
- Oey M.S.: 1996a, *Astrophys. J.*, **465**, 231.
- Oey M.S., 1996b, *Astrophys. J.*, **467**, 666.
- Oey M.S., Smedley S.A.: 1998, *Astron. J.*, **116**, 1263.
- Palouš, J., 1992, in *Evolution of Interstellar Matter and Dynamics of Galaxies*, edited by J. Palouš, W. B. Burton, and P. O. Lindblad (Cambridge Univ. Press, Cambridge), 65.
- Puche, D., Westpfahl, D., Brinks, E. and J-R. Roy, 1992, *Astron. J.*, **103**, N6, 1841.
- Raymond J.C., Smith B.W.: 1977, *Astrophys. J.S.*, **35**, 419.
- Rhode K.L., Salzer J.J., Westpfahl D.J., Radice L.A., 1999, *Astron. J.*, **118**, 323.
- Saken J.M., Shull J.M., Garmany C.D., Nichols-Bohlin J., Fesen, R.A.: 1992, *Astrophys. J.*, **397**, 537.
- Silich S.A., Fomin P.I.: 1983, *Dok. Acad. Nauk SSSR*, **268**, 861.
- Silich S.A.: 1992, *Ap&SS* **195**, 317.
- Silich S.A., Mashchenko S.Ya., Tenorio-Tagle G., Franco J., 1996, *Mon. Not. R. Astron. Soc.*, **280**, 711.
- Silich S.A., Franco J.: 1999, *Astrophys. J.*, **522**, 863.
- Silich, S.A.: 1996, *Astron. Astrophys. Transactions*, **9**, 85.
- Strickland D.K., Stevens I.R.: 1998, *Mon. Not. R. Astron. Soc.*, **297**, 747.
- Tenorio-Tagle G., Palouš J.: 1987, *Astron. Astrophys.*, **186**, 287.
- Tenorio-Tagle G., Bodenheimer P.: 1988, *Ann. Rev. Astron. Astrophys.* **26**, 145.
- Tenorio-Tagle G, Silich S.A., Kunth D., Terlevich E., Terlevich R.: 1999, *Mon. Not. R. Astron. Soc.*, **309**, 332.
- Thilker D.A., Braun R., Walterbos R.: 1998, *Astron. Astrophys.*, **332**, 429.
- van der Hulst J.M.: 1996, in ASP Conf. Ser., **106**, *The Minnesota Lectures on Extragalactic Neutral Hydrogen*, ed. E.D. Skillman, p. 47. Walter F., Kerp J., Duric N., Brinks E., Klein U.: 1998, *Astrophys. J. Lett.*, **502**, L143.
- Wang Q.D.: 1999, *Astrophys. J., Letters* **510**, L139.
- Weaver R., McCray R., Castor J., Shapiro P., Moore, R.: 1977, *Astrophys. J.*, **218**, 377.
- Wrigge M., Wendker H.J., Wisotzki L.: 1994, *Astron. Astrophys.*, **286**, 219.
- Zezas A.L., Georgantopoulos I., Ward M.J.: 1999, *Astro-ph 9903335*.